AAEC/E632

AAEC/E632

AUSTRALIAN ATOMIC ENERGY COMMISSION
RESEARCH ESTABLISHMENT
LUCAS HEIGHTS RESEARCH LABORATORIES

OUT-OF-PILE BURNOUT EXPERIMENTS IN A FULL-SCALE SIMULATION OF AN IRRADIATION RIG IN A HIFAR HOLLOW FUEL ELEMENT FACILITY

by

A.G. CHAPMAN
N.D. HARGREAVES

JUNE 1986

ISBN 0 642 59824 7

AUSTRALIAN ATOMIC ENERGY COMMISSION
RESEARCH ESTABLISHMENT
LUCAS HEIGHTS RESEARCH LABORATORIES

OUT-OF-PILE BURNOUT EXPERIMENTS IN A FULL-SCALE SIMULATION OF AN IRRADIATION RIG IN A HIFAR HOLLOW FUEL ELEMENT FACILITY

by

A.G. Chapman
N.D. Hargreaves

ABSTRACT

Flow measurement and burnout experiments were performed in an out-of-pile test rig which simulates the conditions of a UO_2 irradiation rig in a hollow fuel element facility of the HIFAR reactor. One per cent of the coolant flow in the fuel element passed through the irradiation rig. A burnout heat flux of 90 W cm^{-2} was observed at the surface of an electrically-heated, dummy irradiation can. When the coolant flow rate in the irradiation rig was increased by a factor of 2.5, the burnout heat flux rose by 30 per cent to 117 W cm^{-2}. A simple modification to the supporting frame for the cans improved the burnout heat flux by 3 per cent at 1 per cent of the coolant flow, but enhanced it by 17 per cent at 2.5 per cent of the coolant flow.

Of ten burnout events observed, eight were located upstream of the end of the heated length of the can. The burnout results form a self-consistent, credible set of data and provide a rational basis for the establishment of maximum permissible operating heat fluxes in irradiation rigs of the type simulated. Recommendations are made for the practical application of the results.

National Library of Australia card number and ISBN 0 642 59824 7

The following descriptors have been selected from the INIS Thesaurus to describe the subject content of this report for information retrieval purposes. For further details please refer to IAEA-INIS-12 (INIS: Manual for Indexing) and IAEA-INIS-13 (INIS: Thesaurus) published in Vienna by the International Atomic Energy Agency.

BURNOUT; COOLANTS; CRITICAL HEAT FLUX; EXPERIMENTAL DATA; FLOW RATE; FUEL CANS; FUEL ELEMENTS; HIFAR REACTOR; IRRADIATION CAPSULES; PRESSURE DROP; SIMULATION; URANIUM DIOXIDE; WATER

CONTENTS

1. INTRODUCTION

The HIFAR reactor at the Lucas Heights Research Laboratories (LHRL) is a heavy water cooled and moderated materials testing reactor of the DIDO type. It operates with Mk. IV/VA concentric-tube fuel elements. The hollow centre of a fuel element is occupied by a 54 mm diameter aluminium tube, which is closed at the bottom end by a conical nose cap. The vertical thimble formed by this liner is accessible through the fuel element shield plug and can accommodate suitable targets for irradiation.

At the LHRL, ^{99}Mo is extracted from the fission products of enriched UO_2 pellets that have been irradiated in hollow fuel element (HFE) vertical facilities of the HIFAR reactor. The 9 mm diameter UO_2 pellets are sealed in cylindrical, thick-walled aluminium cans, 143 mm long x 32 mm o.d. At one end the can reduces to a short 16 mm diameter neck where it is cut to allow removal of the irradiated pellets. Up to five cans may be loaded into an HFE facility, supported coaxially within a fuel element liner in a tubular frame. The liner nose cone is perforated by four holes, 3.2 mm diameter, and the liner wall is perforated above the fuel tubes, allowing a small proportion (notionally one to five per cent) of the fuel element coolant flow to bypass the fuel tubes and circulate around the irradiation cans. The arrangement is shown in figure 1.

The fission heat generated in the UO_2 pellets under irradiation produces a moderately high heat flux at the cooled surface of the can and, to avoid the possibility of distortion or failure of a can by overheating, it is necessary to ensure that the critical heat flux is not exceeded. Although the coolant flow passage around the cans is basically annular, it is irregular because the supporting tube has openings for sideways loading and does not completely surround the cans; also, the perforated shelves on which the cans rest produce significant restrictions affecting the distribution of coolant around the cans. It is therefore necessary to determine the critical heat (or burnout heat) flux experimentally. Burnout experiments have been performed using an electrically-heated, dummy irradiation can in an out-of-pile test rig.

The term 'burnout' is used here to describe the advent of the boiling crisis, or the attainment of critical heat flux, regardless of the consequences of this event. Although the term was obviously derived from the destructive consequences that often ensue, in its present usage it no longer signifies that physical damage has occurred.

2. FLOW TESTS

As a first step, an experiment was performed in an out-of-pile test rig to determine the proportion of the fuel element coolant flow that passes through the liner. The test rig is described in Appendix A. A complete full-scale dummy hollow fuel element (HFE), with a perforated liner containing an irradiation rig loaded with five dummy cans, was mounted in a 400 L tank to simulate the reactor arrangement. Measured flows of light water were circulated through the element at 50°C, the normal operating temperature of the reactor coolant. As the liner flow could not be separated for direct measurement, the liner was utilised as a flow meter. First, a series of measurements was made of the pressure drop, between the inlet of the fuel element and a tapping point inside the liner immediately before the outlet holes, at various measured rates of flow through the element. The series was repeated with water temperatures 10°C above and below the normal temperature. The dummy fuel element was then removed from the rig and replaced by the liner alone, still containing the irradiation rig, so that the total measured flow passed through the liner. The arrangement is shown in figure 2. A corresponding set of tests with this arrangement served to establish the relation between the flow rate through the liner and the pressure drop up to the tapping point before the outlet holes.

The overall pressure drop from inlet to tank was not used as the basis for comparison because the flow systems downstream of the liner outlet ports were different. When the liner was tested without the dummy HFE, the final flow passage from the liner outlet ports to the fuel element outlet ports, through the annulus between the liner and the fuel element neck, was absent. The results of these two sets of tests are given in tables 1 and 2. The data are also plotted in figures 8 and 9. For each test in table 2, the measured flow rate in the liner has been expressed as a percentage of the fuel element flow, obtained from figure 8, which corresponds to the same pressure loss in the liner.

It can be seen in figures 8 and 9 that whereas the pressure loss in the HFE decreases as the water temperature is raised, the pressure loss in the liner increases. With rising temperature, friction factors decrease, but flow velocities increase; the effect on the pressure drop depends on whether friction or kinetic effects predominate. Plainly, the pressure drop in the HFE is affected more by friction, but in the liner it is affected more by kinetic effects.

Over the range 8 to 22 kg s^{-1} total light water flow rate through the HFE, the proportion passing through the liner varied between 1.02 and 1.09

per cent, i.e. the proportion was essentially independent of mass flow rate and only very weakly dependent on temperature. This indicates that the proportion of the coolant flow passing through the liner in a heavy water system would be approximately the same as that in the light water system.

It must be understood that, since approximately 87 per cent of the pressure drop through the liner occurs in the nose cone perforations, the proportion of the flow passing through the liner is very sensitive to the size and finish of these holes. As the tests were performed with sharp-edged, accurately drilled holes, the results were expected to indicate the minimum liner flow for the specified design. It is estimated that badly drilled holes (oversize, dulled edge) could probably result in about 35 per cent more flow in the liner, i.e. 1.4 per cent of the flow through the element.

The tests showed that a calculation of the liner flow, based on measured overall pressure drop, was an over-estimation. The calculation had indicated a flow rate in the liner (with perfect nose cone drilling) of 1.4 per cent of the total flow through the HFE. Based on a simplified parallel channel model, in which the theoretical pressure drops in three separate flow paths (see figure 3) were equalised before the restriction at the base of each can, the calculation predicted that 71 per cent of the liner flow would pass through path A, 25 per cent through path B, and 4 per cent through path C, suggesting a grossly non-uniform distribution of coolant flow around the cans. When the different cross-sectional areas were taken into account, the mass flux of coolant in path B was predicted to be 62 per cent of that in path A. The calculations are unconfirmed by experiment; no attempt was made to measure velocities of flow in the various flow paths during the experiments.

3. SIMULATION OF AN IRRADIATION CAN

To facilitate burnout experiments in an out-of-pile rig, an electric heater must be provided to simulate the fission heating in an irradiation can. The most authentic and obvious method would be to insert a sheathed heating element or a resistance winding into an aluminium can in place of the stack of UO_2 pellets. The heating power required to produce the burnout heat flux at the can surface was provisionally estimated to be about 10 kW, but no sheathed heating element of this power and of suitable length could be obtained. Several novel designs of heating element built for laboratory use were examined, but all presented daunting practical problems of uncertain resolution and were therefore discarded.

The required surface heat flux was produced by direct resistance heating of the can wall, using low-voltage direct current. This meant that

only the surface conditions of an irradiation can could be simulated; the electrically-heated counterpart had the same external dimensions and form and a uniform surface heat flux, but the internal heat flows and response to thermal transients were quite different.

Since the purpose of the experiment was to determine the heat flux at the onset of burnout, which is a steady-state phenomenon dependent on surface conditions only, a surface simulation was considered to be satisfactory. This reasoning is similar to that which is followed when electrically-heated, thick-wall steel tubes are used in burnout tests to simulate the fuel rods of reactor fuel elements. The transient processes which follow the onset of burnout, and which depend on the thermal capacity and conductivity of the wall and on the heat source distribution, are not the same in the test as in the reactor. The effect of burnout on the test can cannot, therefore, give an indication of the probable effect of burnout on a thick-wall aluminium irradiation can.

4. DESCRIPTION OF ELECTRICALLY-HEATED TEST CAN (SPLIT SHELL DESIGN)

Substantially large copper conductors are required to supply the low voltage heating current. To preserve the principal external dimensions of the can, the conductors were made of two 'D' section bars, separated by insulation but fitting together to form a cylinder of the same diameter as the neck of an irradiation can (16 mm). To avoid having to provide additional cooling for the conductors, a maximum current of 1100 A was chosen; this gave a resistance of about 0.008 Ω for a 10 kW heater tube of the same external diameter and length as the body of a can. This necessitated material of high resistivity, so stainless steel was chosen because of its ready availability and its suitability for burnout test sections. However, a stainless steel tube of the required resistance and external dimensions has a wall thickness of only 0.09 mm; this is too thin to be of practical use. The tube representing the can was therefore split longitudinally into halves, forming separate electrical paths connected in series by attachment to the circumference of a disk representing the base of the can. The resistor length was thus doubled and its equivalent width halved, allowing the shell wall thickness to be increased to 0.38 mm. In a later design, the wall thickness was increased to 0.76 mm, requiring a current of about 1600 A at 10 kW heating power. Detailed inspection of two typical shells showed the maximum variation from the mean wall thickness (nominally 0.76 mm) to be five per cent. A two-dimensional analysis of the current flow, based on the network of resistances calculated from the measured wall thicknesses, showed the maximum variation from the mean heat flux to be 5.6 per cent.

The construction of the split shell heater is shown in figure 4. Each half shell is attached to a semicircular flange at the end of a supply conductor, shaped to represent the tapered shoulder of a can. The brazing of copper end plates to the stainless steel shell was unsatisfactory owing to the difficulty of ensuring uniform electrical contact; after trying out several other constructions, the final choice was stainless steel end plates, the upper plate being machined integrally with the shell before splitting and the lower being fusion-welded to the shell after the attachment of burnout sensors to the inside surface. The upper plate was bolted to the copper conductor flanges, using a gold shim gasket to improve electrical contact. After assembly of the heater unit, the slits in the shell were temporarily taped over and the hollow interior of the heater was filled with Dow Corning 3120 RTV silicone rubber, a two-part cold-setting compound, poured through a hole in the lower end plate. This filling served to exclude water from the heater interior and to provide insulation between the halves of the shell.

5. METHOD OF BURNOUT DETECTION

It was originally intended to detect the onset of burnout by monitoring the temperature of the heater wall at various points; accordingly, during assembly of the heater, standard chromel-alumel thermocouples were attached to the inside surface of the heater shell by spot-welded saddles, brought out (in Teflon sleeves) through holes in the upper end plate and cone-shaped conductor flanges, and carried alongside the power supply conductors. A maximum of ten thermocouples could be brought through the end plate without serious loss of conduction area.

Owing to the irregularity of the coolant flow channel, the position of the burnout point could not be predicted with confidence. However, burnout was more likely to occur on the surface facing the support tube (see figure 3), where the narrower passage would result in a flow velocity lower than the channel average, and on the upper or downstream part of the can, where the coolant temperature would be higher (these suppositions were later found to be correct). The heater assembly was therefore positioned in the test channel so that one half shell faced the support tube symmetrically, and the majority of the thermocouples were grouped in the upper part of this half shell. Thermocouple signals were displayed on a multi-channel temperature scanner, with trip settings on every channel actuating a heating power trip. During preliminary test runs to check heater operation, the temperature at the inner surface of the heater shell (estimated to be 15°C higher than the outer surface at a heating power of 10 kW) was about

160°C and the trip points were set at 250°C. This method of burnout detection, however, failed to save the heater shell from destruction when burnout occurred, even though the pattern of thermocouple locations was varied in successive replacements of the heater shell. Wherever the thermocouples were placed, visual examination of the burns on the heater shell after a power trip showed that the hot spots skirted the thermocouple locations. It was concluded that since the heater shell was so thin, the heat sink effect of the thermocouples distorted the heat flux distribution sufficiently to influence the position of the burnout point.

Thermocouples of smaller size were not readily available, but after reconsidering the current capacity of the power supply conductors, a current of 1600 A was adopted, which meant that the shell wall thickness could be doubled. Burnout tests performed with the thicker shell wall gave much the same results as with the thinner wall, so the use of thermocouples for monitoring the shell wall temperature was discontinued.

An alternative type of burnout detector, which can be used with direct resistance-heated test sections, is a resistance bridge device which senses the change in electrical resistance of the upper half of the heated wall as its temperature rises. Three voltage tappings are required on the heater wall, one on each half of the upper end plate and one on the lower end plate (centre tapping); the sections between the first and centre, and the centre and last tappings, are connected to opposite sides of the bridge which is balanced by adjusting a compensator. A rapid and substantial departure from balance indicates the onset of burnout in one of the sections and a heating power trip is actuated. The device does not indicate the position of the burnout point within the section. Burnout detectors of this type were developed in England at the Atomic Energy Establishment Winfrith; a similar device, designed and built at Lucas Heights, was used in the experiments which followed the abandonment of wall temperature monitoring. In the split shell heater, each half shell formed a side of the bridge, so that burnout at any location on one side of the heater (usually the side facing the support tube) would be detected.

Although the bridge-type detector was used at its maximum sensitivity, the associated tripping device never succeeded in protecting the heater shell from significant damage during burnout. However, because very fine voltage tapping wires were used, the influence of local heat sinks was removed and the detector gave a positive indication of the onset of burnout and enabled the heating power at burnout to be recorded.

6. PERFORMANCE OF SPLIT SHELL HEATERS

Twelve split shell heaters were used in burnout tests, four with a thin wall and thermocouples, four with a thick wall and thermocouples, and four with a thick wall but no thermocouples. Only one of these yielded useful test results, but it was eventually destroyed during an unplanned oscillation of the coolant flow. All of the others were destroyed in premature and irregular burnouts. Since it is unlikely that any coolant flow irregularity or heater defect could enhance the burnout heat flux, burnout occurring at a heating power significantly lower than that attained in another test at the same nominal conditions was classed as premature. Burnout occurring at a location significantly different from that of other burnouts under the same nominal conditions was classed as irregular.

The burnout damage took the general form of a distinctive bulge in the heater wall, sometimes with a ragged hole where the wall had melted. A common feature of many of the irregular burnouts was an apparent breakdown of the silicone rubber filling beneath the damaged shell and the deposition of a rubber-like substance in the coolant flow channel. It was not known whether the breakdown had occurred during the temperature excursion after the onset of burnout, or whether it happened before burnout, in which case the burnout condition might have been affected. To settle this question, a new heater assembly was mounted in a Perspex tube and placed in a flow of cooling water in a temporary test rig; the assembly could thus be observed while heating power was applied. Although the heater shell was free to expand axially, thermal expansion caused the shell to barrel under heating, because of the restraint of the unheated end plates and the lack of circumferential support. The barrelling widened the slits between the shell halves from 1 mm to about 2 mm at the mid-height; the slits returned to their original size when the heating power was removed. At a heating power a little above 9 kW, the rubber filling began to extrude from the thermocouple lead-in holes and oozed from the ends of the slits, forming a film on the adjacent shell surface. Heating power was removed at this stage; when it was restored, steam bubbles formed under the film and occurred at 8.4 kW burnout, as indicated by a glowing patch under one of the films at the base of the heater.

The test demonstrated the unsuitability of the silicone rubber filling and provided an explanation for the premature and irregular burnouts that had occurred with the split shell heaters, many of which were located at the edge of a slit. In the case of the heater which yielded useful test results, there was no oozing and the heater eventually burned out at a

regular location, i.e. the centre of the half facing the support tube and near the top or downstream end of the heater.

7. DESCRIPTION OF ELECTRICALLY-HEATED TEST CAN (WHOLE SHELL DESIGN)

After the heater demonstration test, the split shell design was abandoned in favour of a whole shell design which completely enclosed the filling. In the first heaters of this design, silicone rubber was still used as a filling, but a test in the demonstration rig showed that the rubber extruded from the joint between the base plate and the lower conductor flange and again spread onto the outer shell surface. In subsequent heaters, the silicone rubber was replaced with Sauereisen Electrotemp cement No. 8, an electrically insulating refractory compound. A demonstration test with a cement-filled heater revealed no unsatisfactory features.

The construction of the whole shell heater is shown in figure 5. To obtain sufficient resistance, a very thin shell wall was required; in a compromise between conductor current restriction and the need to ensure uniformity of wall thickness, a thickness of 0.2 mm was chosen; this required a current of 1700 A to produce a heating power 10 kW. One of the 'D' section conductors was carried through a clearance hole in the upper end plate and passed through the centre of the heater to connect with the lower end plate via a copper flange. Duplicated internal voltage tappings were attached at the shell mid-height to provide the central connection for the bridge-type burnout detector. For the outer connections to the detector and for measurement of the voltage drop across the shell, an internal voltage tapping was attached to the lower end plate and duplicated external tappings were attached to opposite sides of the top end plate.

8. PERFORMANCE OF WHOLE SHELL HEATERS

Twelve whole shell heaters were used in burnout tests. All, without exception, performed satisfactorily. In complete contrast to the inconsistent behaviour of the split shell heaters, burnouts with the whole shell heaters were regular and occurred at the location predicted by theory, i.e. in the upper third of the heated length on the vertical centreline of that side of the shell facing the support tube. None of the burnouts were of the types previously classed as premature or irregular. The initial burnout power levels were sharply defined, and the bridge-type burnout detector gave clear, definite and unambiguous burnout signals throughout all of the tests. Exceptions occurred when heating power was re-applied after the initial burnout trip during tests on the first two heaters; erratic signals were displayed by the burnout detector and the final trip

occurred at a heating power significantly lower than that attained before the initial trip. The burn marks observed after the final power trip were extensive and accompanied by melting. From this it was inferred that the damage sustained by the heater in the initial burnout affected its subsequent performance and only one valid burnout heat flux measurement could be obtained from each heater.

The burn marks that appeared on the shell surface after each initial burnout test were of a regular shape, consistent with growth from a small initial spot. Damage to the shell wall was confined to minor local buckling; no melting occurred in any of the initial burnouts. In one test, the principal axis of symmetry of the burn mark was slightly skewed; in all others it was circumferential, at right angles to the principal direction of coolant flow. In both location and appearance, the burn marks were entirely consistent with the induction of burnout by flow and heat flux alone. There was no indication that any of the initial burnouts might have been affected by the heater construction.

9. METHOD OF CONDUCTING BURNOUT TESTS

Tests were performed using light water coolant at a pressure substantially the same as that of the reactor coolant (helium blanket excess pressure was ignored) in a channel identical to that of an irradition rig in a HIFAR HFE liner. Further tests were performed with a modified can support frame to determine the effect of the modification on the burnout heat flux. The independent variables affecting burnout heat flux are the coolant mass flow rate in the liner and the coolant temperature. Although flow velocity, Reynolds number, and fluid property groups differ in light and heavy water at the same mass flow rate, light water is an acceptable substitute for heavy water in burnout experiments, because experiments with the two liquids in the same annular test sections have indicated that the burnout heat flux in heavy water is slightly higher than that in light water at the same temperature, pressure, and mass flux [Knoebel 1973].

It was not necessary to heat the surface of more than one can in the test assembly, because the high flow resistance imposed by the shelf on which a can rests (estimated to be 14 times as great as that of the pocket containing the can) ensures thorough mixing of the coolant at the base of each can, and the only residual effect of the heating in the preceding cans is a uniform coolant temperature. In the test rig, therefore, only the topmost can was heated, and the effect of irradiation heating in the lower cans was simulated by heating the coolant in an external preheater, before admission to the test channel, to produce the appropriate temperature of

water at the base of the heated can. The topmost dummy can was removed from the support frame and the upper portions of the liner and support tube were cut off just above the level of water in the tank, to permit the insertion of the electrically-heated can to take the place of the topmost can. The arrangement is shown in figure 6.

Burnout experiments were performed in the test rig used for the flow tests. As the proportion of coolant flow passing through the liner had already been determined, simulation of the HFE was unnecessary and all burnout tests were carried out in a simulated liner with a perforated nose cone, containing a can support tube and five cans (one heated). The full measured flow of the test rig was passed through the liner.

The original aim of the experiment was to determine the relation of the burnout heat flux at the surface of a can to the two independent variables of coolant mass flow rate and temperature, a finding which would have enabled accurate predictions to be made of the burnout heat flux at any can in the stack under any coolant conditions. However, a test program to deal systematically with the two variables would have involved a large number of determinations of the burnout power and, in practice, would have relied on an ability to make recurrent tests with the same heater. Since a burnout event invariably resulted in the destruction of the heater, a different approach had to be made.

It was acknowledged that the scope of the investigation would have to be limited to the determination of the burnout heat flux of the topmost can in the most likely loading configuration for an HFE irradiation rig in HIFAR. This limitation eliminated one of the two independent variables, the coolant temperature becoming dependent on the flow rate and the heating power of the top can. Only one burnout determination was then required for each flow rate. With respect to the preferred loading configuration for an HFE irradiation rig in HIFAR, the rig was designed and manufactured with five cans. However, during the project the preferred configuration was changed to a stack of four cans. It was necessary, therefore, to adopt an experimental procedure which did not require alteration to the test rig assembly but was applicable to a stack of four cans. To achieve this, an appropriate proportion of the total heat generation was assigned to the topmost can, and the temperature of the coolant was fixed to that of the inlet to the fourth can.

Before commencing the tests, a calculation was made to estimate the heating distribution among four irradiation cans, under the conditions producing the lowest proportion in the top can. The calculation is repro-

duced in Appendix C. An estimate of the gamma heating in the can support tube and liner was also made; of this, 0.8 was assumed to be absorbed by the coolant before reaching the base of the top can. Then

$$T = T_o + \frac{W}{CM}\left(\frac{1}{\alpha} - 1\right) + \frac{0.8\ W_g}{CM} , \qquad (9.1)$$

where T is the temperature of coolant at base of the top can; T_o is the assumed temperature of coolant at inlet to the fuel assembly; W is the heating power of the top can; C is the specific heat of the coolant; M is the mass flow rate of the coolant; α is the proportion of heat generated in the top can; and W_g is the gamma heating power in the support tube and liner.

The method of conducting a test was to set the rig flow rate at the required amount (M), apply a small heating power (W) to the test can, calculate (T) and raise the temperature of the coolant to this value by means of the rig preheater. Assuming the no burnout was detected, the heating power was raised by a small amount and the coolant temperature increased to the corresponding value. In the course of early tests, the rig was shut down at frequent stages in the power escalation and the heater assembly removed and checked visually to see that no burnout had occurred. This practice was discontinued in later tests, when the consistent performance of the bridge-type burnout detector had confirmed its reliability.

Owing to the erratic behaviour of the split shell heaters, tests with them were conducted cautiously. To obtain the most information before destruction of a heater, the test procedure for each flow rate was performed in stages. At each stage, the power escalation was halted and the process begun at another flow rate; in this way, the burnout powers at three different flow rates were approached in parallel.

10. BURNOUT RESULTS

By the method outlined in section 9, the results given in tables 3 and 4 were obtained from eleven heaters, one of the split shell and ten of the whole shell design. The results of tests on two other whole shell heaters are not included as the test conditions were inappropriate, owing to a lapse in coordination of coolant temperature and can heating power. Table 3 shows the results obtained with the original can support frame, whereas those obtained with a modified frame are shown in table 4. The modification, which was designed to eliminate a severe flow restriction, is shown in figure 7.

Of the twelve split shell heaters tested, only one produced useful results; all others were destroyed in premature or irregular burnouts. The useful results obtained with the split shell heater were the three pre-burnout heat flux measurements given in table 3. This heater was accidentally destroyed during an unplanned flow oscillation, and no valid burnout heat flux measurement was made with it.

Of the twelve whole shell heaters tested, ten produced valid burnout heat flux measurements. Four of these measurements were made using the original can support frame and six were made using the modified design. Coolant flow rate in these tests ranged from 0.15 to 0.375 kg s^{-1}, i.e. from 1 to 2.5 per cent of the nominal flow rate in an HFE. In each test, the coolant temperature was adjusted to correspond to the predicted temperature at the base of the topmost irradiation can in a stack of four cans in a HIFAR HFE UO_2 irradiation rig, with coolant entering the fuel element at 50°C.

The variation of burnout heat flux with coolant flow rate in the fuel element liner, for the two types of can support frame, is shown in figure 10. The location of the burnout point, though always on the centreline of the side of the shell facing the support tube, varied in axial position between 0.61 and 0.82 of the heated length when the original support frame was used, and between 0.64 and 0.94 when the modified support frame was used.

11. DISCUSSION

11.1 Effect of Coolant Flow Rate

In these burnout tests, the normally independent variables of coolant flow rate and coolant inlet temperature were associated, and varied simultaneously in accordance with equation 9.1. As a consequence, the inlet temperature at burnout decreased with increasing flow and the results, shown in figure 10, do not follow the familiar trend of burnout heat flux when flow rate is the sole influence. In the present tests, the burnout heat flux increased at a growing rate as the coolant flow in the liner was increased from 1 to 2.5 per cent of the nominal flow in an HFE.

In the tests, the coolant flow rate was increased by raising the pressure at which it was supplied to the inlet of the test section. In the reactor, an increase in the flow rate in the liner can be effected only by reducing the flow resistance of the liner and thereby increasing the proportion of coolant diverted from the HFE. This requires a physical alteration to the liner, changing the size or number of the perforations. In the flow tests the pressure loss over the liner nose cone perforations,

with 1 per cent of the total fuel element flow passing through the liner, was about 87 per cent of the loss over the whole liner. If the flow resistance of the nose cone were totally removed by making large openings in the case, the flow rate in the liner would increase in the ratio of approximately the square root of 1.0/(1.0-0.87), or 2.7, to produce the same loss over the whole liner. Any flow rate within the range covered by the burnout tests, from 1.0 to 2.5 per cent of the nominal flow in an HFE, can therefore be achieved in the reactor.

The effect simulated in these tests was that of flow regulation by adjustment of the flow resistance of the liner nose cone perforations. Of the two methods that could be used, this has the more adverse influence on the burnout heat flux, because a severe flow restriction at the inlet of the channel produces a disturbing effect which could persist in some degree throughout the channel and, more certainly, it reduces the coolant pressure at the burnout point. A reduced pressure means a smaller degree of subcooling at a given coolant temperature, hence a lower burnout heat flux. The preferable alternative is to place the flow regulating restriction at the liner outlet perforations, avoiding disturbances in the channel and raising the pressure at the burnout point. If the flow resistance of approximately 23 kPa, required to restrict the liner flow to 1 per cent of the total HFE flow, were placed at the liner outlet instead of at the inlet, the saturation temperature of the coolant would be raised by more than 5°C, producing an increase of nearly 50 per cent in the inlet subcooling at the topmost can at burnout.

Calculations to determine the size and number of perforations required in the liner to produce a desired flow rate may be carried out as if the coolant were ordinary water, provided that the expected overall pressure loss matches the fuel element pressure loss in ordinary water. With the same volume flow rates of heavy water, the pressure losses in both the HFE and liner will be greater, but remain practically equal. Figure 8 shows the pressure difference in a fuel element at various flow rates of ordinary water. Once the nominal flow rate in the fuel element is chosen, it is checked against the figure to indicate the pressure loss that the liner should be designed to produce when passing the required flow rate. The calculations can be based on a uniform flow distribution, since the sections affected by non-uniform flow contribute very little to the overall pressure loss.

11.2 Location of the Burnout Point

In undisturbed flow, the onset of burnout should occur on the vertical

centreline of the side of the can facing the support tube, where there is a low point in the coolant flow distribution, and near the flow outlet end of the heated length, where the coolant enthalpy is at its highest. At burnout, the surface hot spot should form a short distance from the end of the thin-walled shell of the heater, because the thick end plate acts as a heat sink. In fact, although all of the observed burnouts occurred in the expected circumferential location, only two were in the expected axial location; the remainder were what are commonly termed 'upstream' burnouts. This is not surprising; on a uniformly-heated surface, the position of the point of onset of burnout is affected by flow disturbances which can produce higher than average local enthalpies by setting up small recirculation cells. Upstream burnout is quite common in rod bundle and annular channels in which the flow is disturbed by a rod support grid near the outlet end. In the present case, the prevalence of upstream burnouts is an indication of the disturbed nature of the flow, arising from the obstruction created by the support shelf at the base of a can and the polar asymmetry of the channel.

In the tests made with the modified support frame, there was a tendency for the location of the burnout point to shift towards the flow inlet end of the heated length as the flow rate and the burnout heat flux increased. The smaller number of tests made with the original support frame (which offered a greater flow obstruction at the can support shelf) did not establish a definite trend in the axial location of burnout, but at all flow rates except the highest, burnout occurred nearer the inlet. Since it can be presumed that the more a burnout is affected by flow disturbances the nearer to the inlet it will occur, it can be inferred first, that the improvement achieved in burnout heat flux by increasing the flow rate is impaired to some extent by increased disturbance. Second, the higher burnout heat fluxes attained with the modified frame are due, at least in part, to reduced disturbance, although the main purpose of the modification was to improve the supply of coolant to the critical flow path.

In both types of support frame, the access openings in the support tube are larger at the top end of the can than at the bottom; the enlargement occurs at about 0.7 of the heated length of the test can (see figure 1). The fact that most of the upstream burnouts occurred at between 0.7 and 0.83 of the heated length leads to the supposition that a disturbance pattern, such as a vortex, might originate at the enlargement and extend circumferentially around the can.

11.3 Effect of Boiling

At one per cent flow (0.15 kg s^{-1}), the lowest flow rate at which a valid burnout was recorded, bulk boiling conditions existed at the test channel exit when the burnout power was reached. The pressure at the test channel exit, which was near the surface of the water in the bank, was between 8 and 12 kPa lower than at the end of the heated can, depending on the coolant flow rate. In tests with a split shell heater at 0.8 per cent flow (0.12 kg s^{-1}), exit bulk boiling occurred at the highest pre-burnout powers attained. If bulk boiling were to occur at the heated section, it should appear first in the space between the can and the support tube (flow path B in figure 3), where the flow is constricted; an unstable condition would then be likely to develop as the increased pressure drop due to the two-phase state would cause a diversion of coolant from the boiling flow path and increased vapour generation in this path. This leads to the hypothesis that burnout is induced by flow instability following the onset of bulk boiling.

The two straight lines drawn on figure 10 represent the heated can surface heat flux required to produce a saturated condition of the coolant at the end of the heated length, based on two different assumptions regarding the degree of mixing around the can, i.e. between flow paths A and B (see figure 3). The upper line relates to perfect mixing, the lower to no mixing. The actual threshold must lie between these two lines. Since mixing is complete when the coolant reaches the channel exit, the heat flux must lie near the upper line to produce exit bulk boiling. This prediction is confirmed by the observations of exit bulk boiling before burnout at flow rates of 1 and 0.8 per cent of the nominal HFE flow rate.

If all of the burnout points obtained with the modified support frame were given equal credence, the curve drawn through them (see figure 10) intersects the lower saturation line at 1.85 per cent flow and follows the saturation line between this and the 1.5 per cent flow, seemingly supporting the hypothesis that burnout is induced by flow instability at low flow rates. However, the burnout heat flux at 1.0 per cent flow is well above the lower saturation line, and the possibility of a corresponding irregularity in the results obtained with the original support frame is highly conjectural. It is concluded, therefore, that the high burnout heat flux observed at 1.73 per cent flow is a freakish result arising from a fortuitous absence of the usual flow disturbances, a conclusion that is supported by the unusual location of the burnout point near the end of the heated length.

11.4 Effect of Support Frame Modification

The support frame consisted of a vertical tube closed at the bottom end by a conical nose cap, and divided axially into five compartments by four transverse plates. Openings were provided in the wall of each compartment for the insertion or removal of irradiation cans, which rested in the compartments on the shelves formed by the dividing plates. The nose cap and dividing plates were perforated to allow coolant to flow through the compartments; the restriction at each plate imposed a flow resistance many times greater than that of a compartment. This restriction between compartments had a beneficial effect; it assisted mixing of the coolant before entry to the next compartment and inhibited carry-over of an adverse temperature profile arising from non-uniform flow distribution around the preceding can.

The modification affected the size and arrangement of the perforations in the dividing plates (see figure 7). In the original design, slots in the plate directed the coolant to a space under the base of the can above, from which it flowed radially through narrow slots between the base of the can and its seat. The radial entry into a compartment encouraged the formation of a strong cell of recirculating flow at the lower end of the can, and high velocity jets issuing from the narrow slots created a highly disturbed flow. In the modified design, relatively large axial slots in the dividing plate admitted coolant directly to the annular passage surrounding a can; radial flows were not generated and velocity changes were less severe. The flow resistance of the modified dividing plate was lower than that of the original, but it was sufficient to enable a beneficial mixing action.

When the support frame was replaced by the modified frame, the burnout heat flux increased at every flow rate between 1.0 and 2.5 per cent of the nominal fuel element coolant flow. At the lower end of the flow range, the improvement was 3.7 per cent, but this increased to 17.4 per cent at the highest flow rate. The greater improvement at the higher flow rates was consistent with the theory of reduced levels of flow disturbance with the modified frame; a lower degree of disturbance enabled the benefits of higher flow rate to be more fully realised.

11.5 Consequences of Burnout

The term 'burnout' is used in this report to describe the advent of the boiling crisis and has no necessary significance in respect to the consequences of this event. The consequences depend on the response of the heat transport system to the event.

In the tests, heat was generated very close to the cooled surface in a thin layer of material of moderate thermal conductivity. When the critical heat flux was reached at a small spot on the surface, the characteristic sudden and substantial reduction in cooling heat transfer all but closed the only effective path for the heat generated, resulting in a sudden rise in the temperature of the layer of material at that spot. The only alternative transport path for this heat is by conduction parallel to the surface and requires a very high temperature gradient. The temperature rise at the hot spot was sufficient to distort or, in some cases, melt the material. The rapid rise in temperature at burnout was an advantage in the tests because it provided a sharp definition of the burnout point and allowed a very precise measurement of the burnout power to be made.

In the real irradiation can the situation is very different, since heat is generated in the core and conducted to the cooled surface through a thick wall of aluminium, which has good thermal conductivity and forms a heat distributing medium between the heat source and the heat sink. If the critical heat flux were to be reached at a spot on the surface, a small rise in the temperature of the spot would be sufficient to redirect the heat flow to adjacent areas. If the critical heat flux condition was due to a small local disturbance in the coolant flow, the slight increase in the heat flux at the adjacent surface would not cause the condition to spread and the effect would scarcely be noticeable. In fairly uniform coolant conditions, however, the affected area would spread until the boundary met with conditions that were sufficiently different to support nucleate boiling at the required heat flux.

The larger the affected area, the greater would be the effect on temperature distributions within the can; these could be destructive if the area extended over a large portion of the total surface of the can. What is emphasised, however, is that the fate of the test cans in no way illustrates the consequences of the heat flux attaining the critical value at a point on the surface of a real irradiation can. Immediate failure of a real can is highly improbable, and in some circumstances no damage whatsoever would be sustained.

11.6 Significance of the Method of Testing

The number of tests required was reduced to a minimum by considering only one independent variable, the coolant flow rate. The only other condition that can vary significantly under reactor operating conditions is the temperature of the coolant at the base of the can; this was made dependent on the flow rate and the can heating power by assuming a fixed can

position and a coolant temperature of 50°C at the inlet to the HFE. The test can represented the top can in a stack of four, and throughout the tests the coolant was supplied to this can at the appropriate temperature. It is important to understand that the variation of coolant temperature was not an independent effect, consequently a general relation between burnout heat flux and coolant temperature cannot be deduced from the results.

The significance of this restricted method of testing is that the results apply strictly to the top can in a stack of four, and not to a can in any other position. The burnout heat flux for a can in a lower position (i.e. with less than three preceding cans) would be higher than that determined in a test, because the coolant temperature would be lower. This effect of coolant temperature has been established in countless burnout experiments and does not require further demonstration. However, the results of the tests do not quantify the dependence of burnout heat flux on the coolant temperature and therefore do not indicate how much higher the burnout heat flux would be. It is clearly possible for burnout to appear in the third can of a stack of four before it appears in the top can, because the neutron flux, and hence the heat flux at the can surface, is higher in the third can. This does not detract from the usefulness of these results, for the tests establish a lower bound of the burnout heat flux for a can in any position; if the onset of burnout occurs on the third can of a stack of four, or on the second or third can of a stack of three, it will be at a heat flux higher than that observed in the tests. Similar reasoning can be applied quite properly when considering the temperature of the coolant at the inlet to the HFE. The temperature to which the tests relate is the normal maximum of 50°C; with any lower coolant inlet temperature burnout would occur at a heat flux higher than that observed in the tests.

11.7 Effect of the Heated Surface Area

The calculation of burnout heat flux from the measured burnout power was based on the effective heated surface area of the test heater, which was 81.4 cm^2. This is somewhat less than the external cylindrical surface area of the main barrel of a real irradiation can.

If the burnout heat flux can be related to the temperature of the coolant at the burnout point, there is no effect from the heated surface area. However, it is well known that when burnout is related to the coolant inlet temperature and occurs at the exit of a uniformly-heated channel, the burnout heat flux and the burnout power are dependent on the heated surface area, because this determines the coolant enthalpy at the burnout

point. The greater the surface area, the lower is the burnout heat flux, but the higher the burnout power. In the case of upstream burnout, the situation is not as clear, because the enthalpy at the burnout point is more dependent on the local disturbance than on the total surface area. It would be prudent, however, to assume that upstream burnout heat fluxes and powers are affected in the same way as exit burnout conditions.

Burnout heat fluxes in the tests cannot be accurately related to the coolant temperature at the burnout point, because the mass distribution of coolant around the can is not precisely known and the reheating effects of recirculating cells in the coolant flow are totally unknown. The effect of heated surface area must therefore be considered. Although the split shell heaters used in earlier tests had a greater effective heated surface area, they did not yield burnout results that were suitable for comparison with results from the whole shell heaters. Hence, there is no indication of the magnitude of the effect of surface area on burnout conditions. However, the results established a lower bound of burnout heat flux for heated surface areas of less than 81.4 cm^2, and a lower bound of burnout power for heated surface areas greater than 81.4 cm^2. If the results are used to predict burnout heat flux on a can with an effective heated surface area greater than 81.4 cm^2, the value for observed burnout heat flux should be adjusted by multiplying it by the ratio of the effective heated surface areas of test can to real can.

11.8 Uncertainty in Prediction of Burnout Heat Flux

A prediction of the burnout heat flux in an irradiation rig may be made by estimating the coolant flow rate in the liner and then referring to the appropriate curve in figure 10. The principal uncertainties are from possible errors incurred when estimating the flow rate and those arising from the unpredictable effects on burnout heat flux of random disturbances in the flow.

The effect of an error in the estimation of the flow rate is indicated by the slope of the curves in figure 10. The greatest effect is at high flow rates with the modified support frame; in this region the slope of the curve yields the following relation between the proportional change in burnout heat flux ($\Delta\phi/\phi$) and the proportional change in mass flow rate ($\Delta M/M$):

$$(\Delta\phi/\phi)_M = 0.8\ (\Delta M/M)$$

It is reasonable to assume that the flow rate in the liner can be estimated within an accuracy band of ±25 per cent (which implies estimating the pressure loss within ±50 per cent). The limits of $\Delta M/M$ are then ±0.25 and

the limits of $(\Delta\phi/\phi)_M$ are ±0.20, i.e. the predicted burnout heat flux could be in error by 20 per cent owing to an error in estimating the flow rate.

The curves drawn in figure 10 are lower envelopes of the test points; they make some allowance, therefore, for the scatter produced by random effects of flow disturbances. However, the number of tests is too small to indicate the probable extent of the scatter and it must be accepted that a chance flow irregularity could cause a burnout heat flux value to fall below the relevant curve. The root mean square (r.m.s.) value of the deviations of the test points from the curves is four per cent; it is unlikely that any point would fall below the curve by more than twice this amount, bearing in mind that the curves are drawn through the lowest test points. The maximum negative proportional deviation of burnout heat flux from the curve, due to flow irregularity $(A\phi/\phi)_I$), is therefore likely to be -0.08.

The correction factor to be applied to the predicted burnout heat flux, to allow a margin for possible error in the estimation of the flow rate in the liner and for possible effects of flow irregularity, is given by

$$1 + \frac{\Delta\phi}{\phi}_T = 1 + \frac{\Delta\phi}{\phi}_M \; 1 + \frac{\Delta\phi}{\phi}_I$$

Insertion of the maximum negative values of $(\Delta\phi/\phi)_M$ and $(\Delta\phi/\phi)_I$ gives

$$(1 + \frac{\Delta\phi}{\phi})_T = 0.80 \times 0.92 = 0.74$$

The corresponding burnout margin is the reciprocal of this factor, i.e. 1.36. The burnout margin is the ratio of the predicted burnout heat flux to the maximum safe operating heat flux.

12. CONCLUSIONS

The main findings of the investigation are summarised below; the sections and tables in which these findings are discussed are given in parentheses. Except where differences are expressly mentioned, all values of burnout heat flux relate to the standard set of conditions listed in Appendix B, for a can having an effective heated surface area of 81.4 cm^2 or less, and occurring at the surface of the topmost can in a stack of four active cans.

In a Mark 4/5A HIFAR HFE, with a standard perforated liner containing an irradiation rig loaded with five cans, 1.05 per cent of the total flow of coolant passes through the liner. This proportion remains constant over

a range of flow rates between 0.5 and 1.5 times higher than the nominal flow in an HFE, and practically constant over a range of coolant temperatures between 40 and 60°C. The proportion is the same for both ordinary and heavy water coolants (section 2).

The burnout events were sharply defined and unambiguous. There is no reason to believe that they were affected by any condition that was not a reasonable simulation of operating conditions in an irradiation rig in the reactor (section 8).

After reasonable allowances for experimental error and the random nature of flow disturbances, the burnout results constitute a self-consistent, credible set of data and provide a rational basis for the establishment of maximum permissible heat fluxes in irradiation rigs of the type tested (section 11).

Upstream burnout is typical of burnout behaviour in the irradiation rig channels (section 11.2).

Under the standard set of conditions, the burnout heat flux is 90 W cm^2 (table 3).

At a coolant flow rate of 0.375 kg s^{-1} in the liner (2.5 times the standard flow rate) the burnout heat flux is 117 W cm^{-2}, 30 per cent higher than at the standard flow rate (table 3).

When the can support frame is changed to the modified design (see figure 7), the burnout heat flux is raised to 93 W cm^{-2}, three per cent higher than with the standard design (table 4, section 11.4).

When the can support frame is changed to the modified design and the coolant flow rate in the liner is increased to 0.375 kg s^{-1} (2.5 times the standard flow rate), the burnout heat flux is raised to 137 W cm^{-2}, 17 per cent higher than at the same flow rate with a standard support frame, and 47 per cent higher than at the standard flow rate with a modified support frame (table 4, section 11.4).

When a can has an effective heated surface area 5 cm^2 greater than 81.4 cm^2, the burnout heat flux may be reduced, but is not less than 81.4/86.4 times the burnout heat flux at the surface of a can with an effective heated surface area of 81.4 cm^2 (section 11.7).

The burnout heat flux at the surface of any can other than the topmost in a stack of four is greater than that at the surface of the topmost can (section 11.6).

The burnout heat flux at the surface of any can in a stack of fewer than four cans is greater than that at the surface of the topmost can in a stack of four (section 11.6).

13. RECOMMENDATIONS

A number in brackets is a reference to the section of this report in which the basis of the recommendation is discussed.

The burnout heat flux at the surface of a UO_2 irradiation can in a HIFAR HFE facility should be predicted by reference to the appropriate curve in figure 10, using an estimated flow rate of coolant in the liner. For a can which has an effective heated surface area 5 cm^2 more than 81.4 cm^2, the predicted burnout heat flux should be corrected in the ratio 81.4:86.4 (section 11.7).

A burnout margin of 1.4 should be applied to allow for possible error in the estimation of coolant flow rate and for the possible effects of chance irregularities in the flow (section 11.8).

Any flow restriction introduced for the purpose of regulating the coolant flow rate in the liner should be placed at the liner outlet, to maintain the highest possible pressure of the coolant inside the liner (section 11.1).

The size and number of perforations required in the liner should be determined from a calculation of the pressure loss in the liner with the desired coolant flow rate, treated as ordinary water. The required overall pressure loss should be obtained by reference to figure 8, using the nominal coolant flow rate in the fuel element. A uniform distribution of flow in the liner may be assumed for the calculations (section 11.1).

14. ACKNOWLEDGEMENTS

The experiments were performed under the general direction and guidance of Mr W.J. Green. Throughout the practical work of servicing and operating the experimental rig, the authors received willing assistance from Mr D. Paton. In the final stages of the experiment Mr W.J. Crawford deputised for Mr Hargreaves in a most able and competent manner. During the early endeavour to produce a compact heating element to simulate a stack of UO_2 pellets, Mr V. Cornford built a working prototype of a heated can which helped to demonstrate the power limitations of such designs. The investigation was assisted at several stages by helpful discussions with staff from the Commercial Products Unit and HIFAR Operations Section; the latter also provided essential information and materials.

15. REFERENCES

Knoebel, D.H., Harris, S.D., Crain, B. Jr., Biderman, R.M. [1973] - Forced convection subcooled critical heat flux. DP-1306.

TABLE 1

FLOW-PRESSURE LOSS TESTS ON DUMMY MARK 4/5A FUEL ELEMENT WITH STANDARD PERFORATED LINER AND IRRADIATION RIG

Test fluid: demineralised ordinary water.
Pressure drop excluding change in static head.

Water Temp. (°C)	Flow Rate (kg s^{-1})	Pressure Drop Between Inlet and Station (kPa)			
		Inside Liner			Tank
		Downstream of Nose Cone	Centre of Rig	Upstream of Outlet	
40	8.01	9.07	10.42	10.73	10.85
	9.91	13.71	15.59	16.08	16.30
	11.95	21.16	23.55	24.14	24.60
	13.12	25.74	28.32	29.06	29.58
	13.95	28.87	31.52	32.35	32.93
	15.95	37.70	40.68	41.70	42.50
	17.94	47.32	50.68	51.97	52.92
	19.94	57.78	61.35	62.85	64.18
	21.86	69.53	73.52	75.00	76.69
50	7.95	8.92	10.09	10.46	10.55
	9.96	14.27	16.02	16.48	16.70
	11.92	20.23	22.48	23.09	23.52
	13.10	24.32	26.78	27.46	28.04
	13.92	27.49	30.01	30.75	31.43
	15.92	36.10	38.96	39.88	40.65
	17.89	45.91	49.02	50.25	51.29
	19.90	56.89	60.24	61.72	63.13
	21.91	69.03	72.91	74.60	76.17
60	7.93	8.49	9.69	9.96	10.15
	9.87	13.16	14.85	15.25	15.56
	11.90	20.33	22.60	23.28	23.71
	13.07	24.38	26.91	27.58	28.14
	13.89	27.31	29.77	30.63	31.37
	15.88	35.49	38.35	39.33	40.19
	17.78	44.93	48.06	49.17	50.28
	19.84	55.10	58.49	59.87	61.35
	21.79	66.14	70.14	71.59	73.34

NOTE: Each value in the table is the average of two measurements made at the same conditions.

TABLE 2

FLOW-PRESSURE LOSS TESTS ON LINER AND IRRADIATION RIG ONLY

Test fluid: demineralised ordinary water.
Pressure drop excluding change in static head.

Water Temp. (°C)	Flow Rate ($kg\ s^{-1}$)	Pressure Drop Between Inlet and Station (kPa)				Flow Rate as Proportion of that in Fuel Element at Same Liner Loss (%)
		Inside Liner			Tank	
		Downstream of Nose Cone	Centre of Rig	Upstream of Outlet		
40	0.074	7.13	7.69	7.81	8.24	1.08
	0.092	10.70	11.99	12.05	12.18	1.08
	0.107	14.64	16.11	16.36	16.54	1.08
	0.121	18.82	20.60	21.03	21.34	1.08
	0.139	24.66	26.94	27.43	27.61	1.09
	0.153	29.83	32.53	32.90	33.33	1.09
	0.171	36.90	39.91	40.47	40.96	1.09
	0.187	44.46	47.72	48.22	48.77	1.08
	0.202	51.66	55.10	55.97	56.46	1.08
	0.220	61.01	64.94	65.81	66.60	1.08
50	0.078	8.06	8.79	8.98	9.00	1.06
	0.086	9.78	10.76	11.07	11.09	1.05
	0.088	10.21	11.32	11.44	11.46	1.06
	0.109	15.56	17.16	17.47	17.50	1.05
	0.122	19.50	21.34	21.96	22.00	1.05
	0.138	25.03	27.24	27.98	28.02	1.05
	0.153	30.69	33.27	33.95	34.00	1.05
	0.168	37.15	40.10	40.96	41.02	1.04
	0.186	45.26	48.40	49.57	49.63	1.05
	0.201	52.83	56.21	57.63	57.69	1.05
	0.217	61.62	65.19	66.73	66.79	1.05
	0.234	70.91	74.85	76.88	76.94	1.05
60	0.060	4.74	5.29	5.60	5.60	1.04
	0.076	7.63	8.55	8.86	8.88	1.04
	0.089	10.76	11.87	12.24	12.26	1.05
	0.106	15.01	16.48	16.97	17.00	1.04
	0.120	19.25	21.09	21.65	21.68	1.04
	0.138	25.77	28.17	28.84	28.88	1.03
	0.154	31.98	34.44	35.55	35.59	1.02
	0.168	37.88	41.02	41.94	41.99	1.02
	0.185	45.69	48.95	50.12	50.18	1.02
	0.203	54.67	58.06	59.72	59.78	1.02
	0.217	62.73	66.05	67.65	67.72	1.02
	0.231	70.54	74.35	76.26	76.34	1.02

TABLE 3

BURNOUT RESULTS FOR SIMULATED IRRADIATION RIG
WITH ORIGINAL CAN SUPPORT FRAME

Heater	Coolant Flow Rate ($kg\ s^{-1}$)	Coolant Temp. at Inlet to Fourth Can (°C)	Coolant Pressure at Top of Fourth Can (3) (bar)	Coolant Saturation Temp. (°C)	Inlet Subcooling at Fourth Can (°C)	Burnuut Power (kW)	Burnout Heat Flux (4) ($W\ cm^{-2}$)	Location of Burnout Point Proportion of Heated Length
M7 (1)	0.115	96.8	1.094	102.1	5.3	6.871 (2)	77.9 (2)	-
M7 (1)	0.150	92.3	1.097	102.2	9.9	7.779 (2)	88.2 (2)	-
M7 (1)	0.223	80.2	1.106	102.5	22.3	8.530 (2)	96.7 (2)	-
M13	0.148	89.2	1.097	102.2	13.0	7.332	90.1	0.70
M15	0.226	77.8	1.106	102.5	24.7	7.950	97.7	0.73
M24	0.302	74.2	1.117	102.8	28.6	9.060	111.3	0.61
M23	0.376	70.2	1.131	103.1	32.9	9.515	116.9	0.82

NOTES: (1) Split shell heater.

(2) Pre-burnout condition.

(3) Coolant pressure calculated from depth of immersion and estimated losses downstream of top of fourth can.

(4) Burnout heat flux calculated from effective heated surface area of test can:
split shell heater 88.2 cm^2
whole shell heater 81.4 cm^2

TABLE 4

BURNOUT RESULTS FOR SIMULATED IRRADIATION RIG
WITH MODIFIED CAN SUPPORT FRAME

Heater	Coolant Flow Rate ($kg\ s^{-1}$)	Coolant Temp. at Inlet to Fourth Can (°C)	Coolant Pressure at Top of Fourth Can (1) (bar)	Coolant Saturation Temp. (°C)	Inlet Subcooling at Fourth Can (°C)	Burnout Power (kW)	Burnout Heat Flux (4) ($W\ cm^{-2}$)	Location of Burnout Point Proportion of Heated Length
M17	0.153	90.3	1.097	102.2	11.9	7.605	93.4	0.94
M18	0.225	78.9	1.106	102.5	23.6	8.219	101.0	0.81
M21	0.260	79.3	1.110	102.6	23.3	9.704	119.2	0.92
M19	0.302	76.1	1.117	102.8	26.7	9.870	121.2	0.83
M22	0.338	74.4	1.124	102.9	28.5	10.607	130.3	0.81
M20	0.372	74.0	1.130	103.1	29.1	11.184	137.4	0.64

NOTES: (1) Coolant pressure calculated from depth of immersion and estimated losses downstream of top of fourth can.

(2) Burnout heat flux calculated from 81.4 cm^2 effective heated surface area of test can.

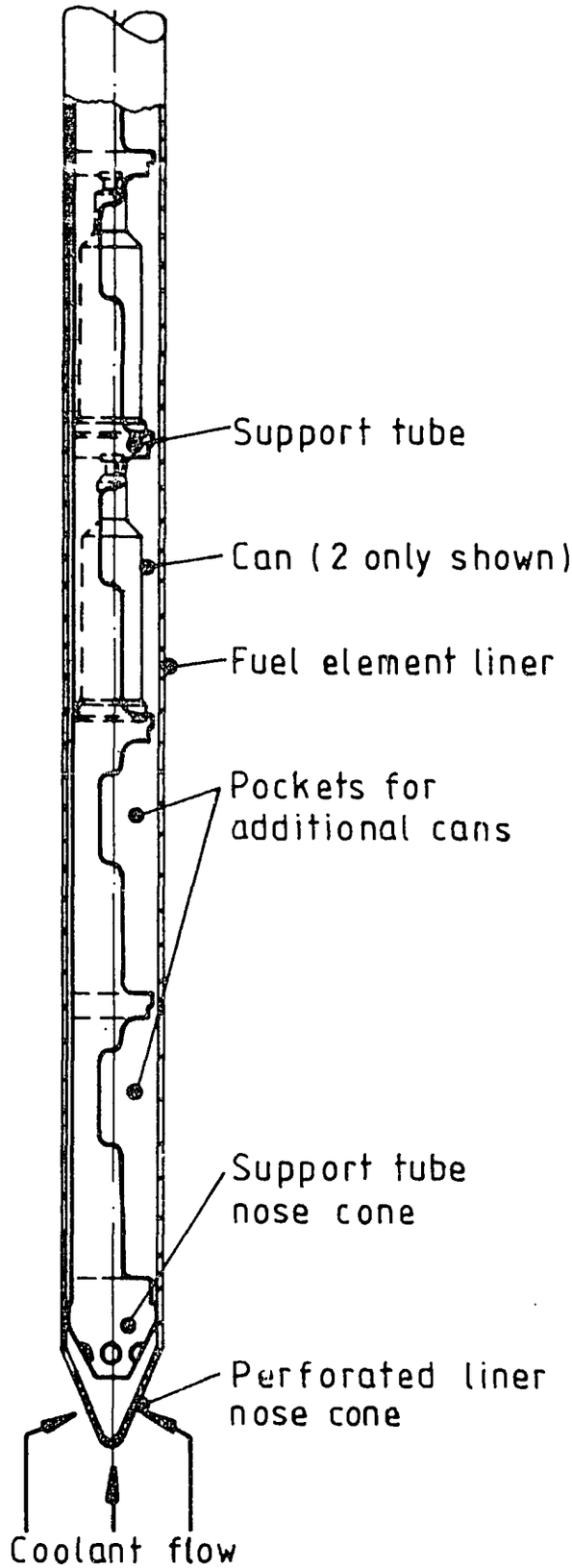

Figure 1 Section through fuel element liner showing arrangement of HIFAR HFE irradiation rig

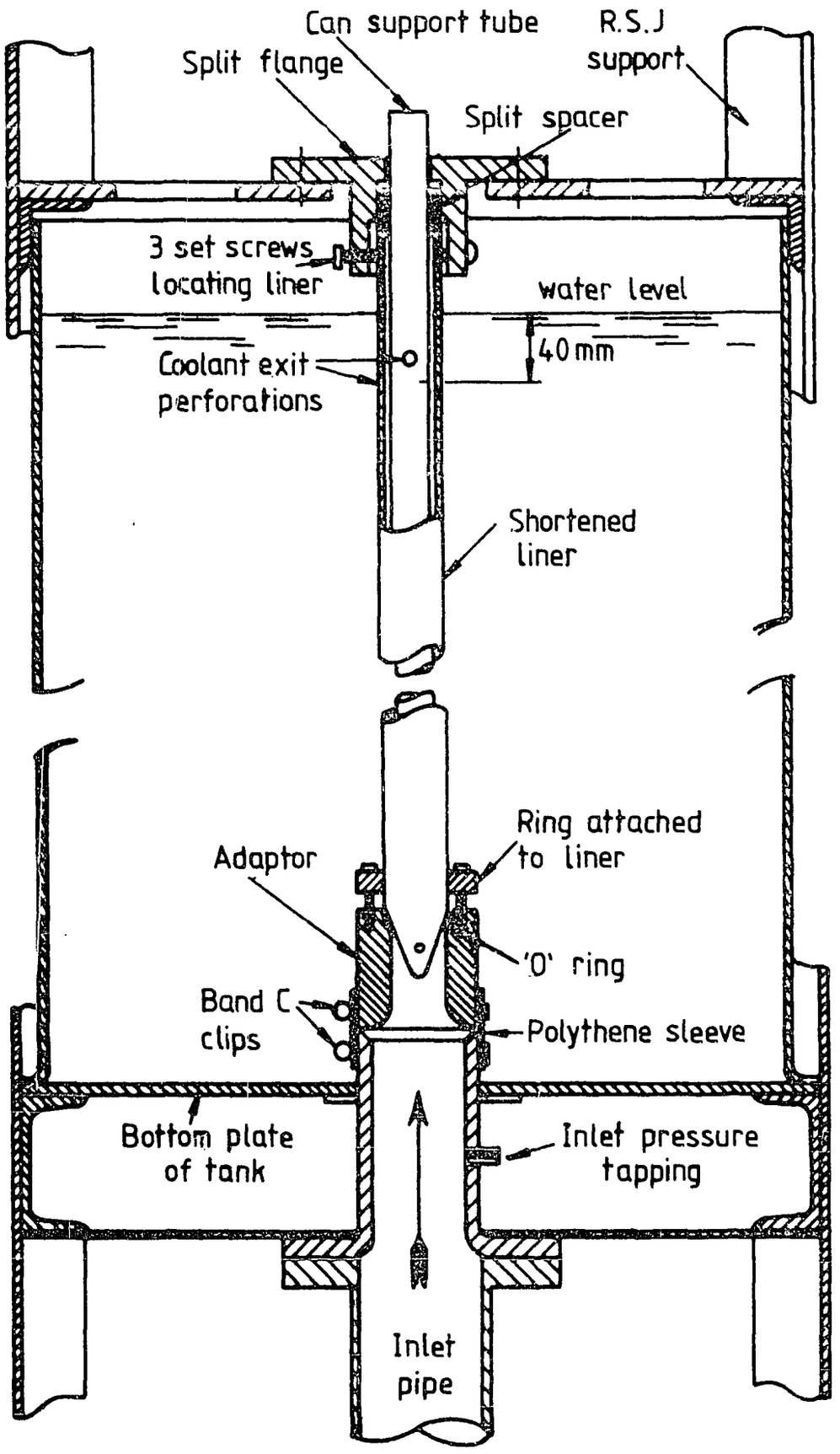

Figure 2 Arrangement of liner in test rig (without dummy fuel element)

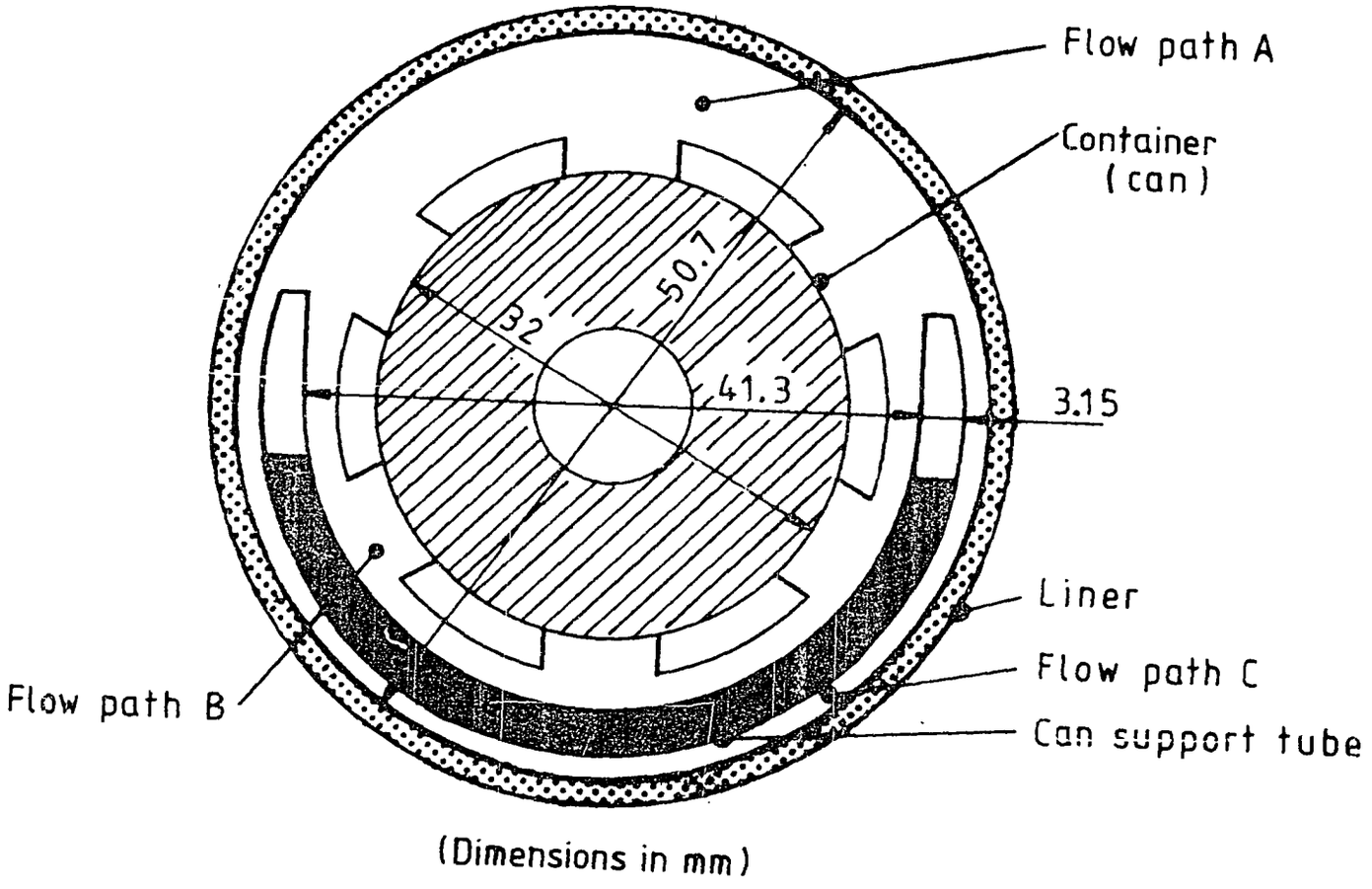

Figure 3 Cross-section of irradiation assembly at location of burnout

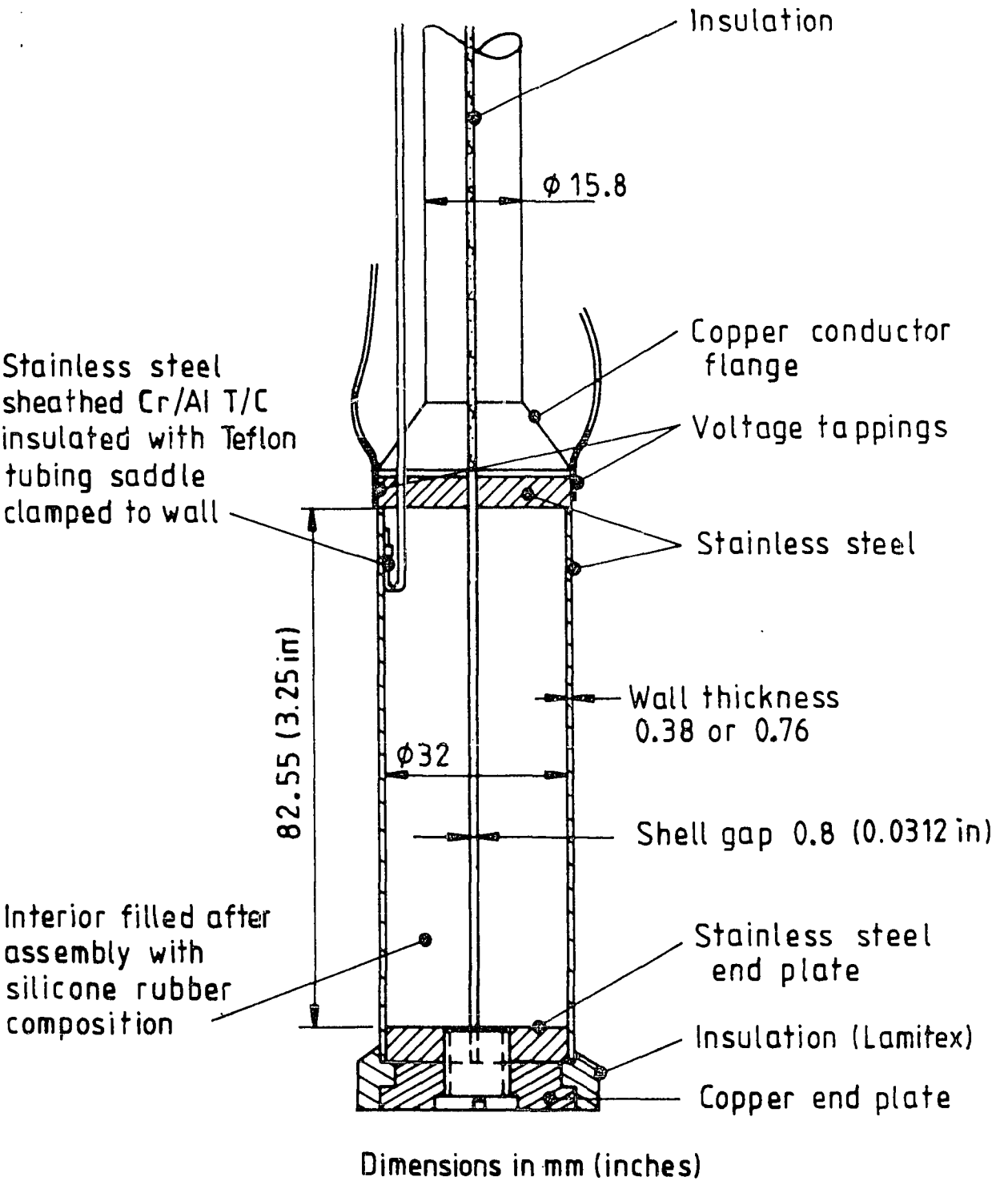

Figure 4 Electrically-heated simulation of irradiation can (split shell design)

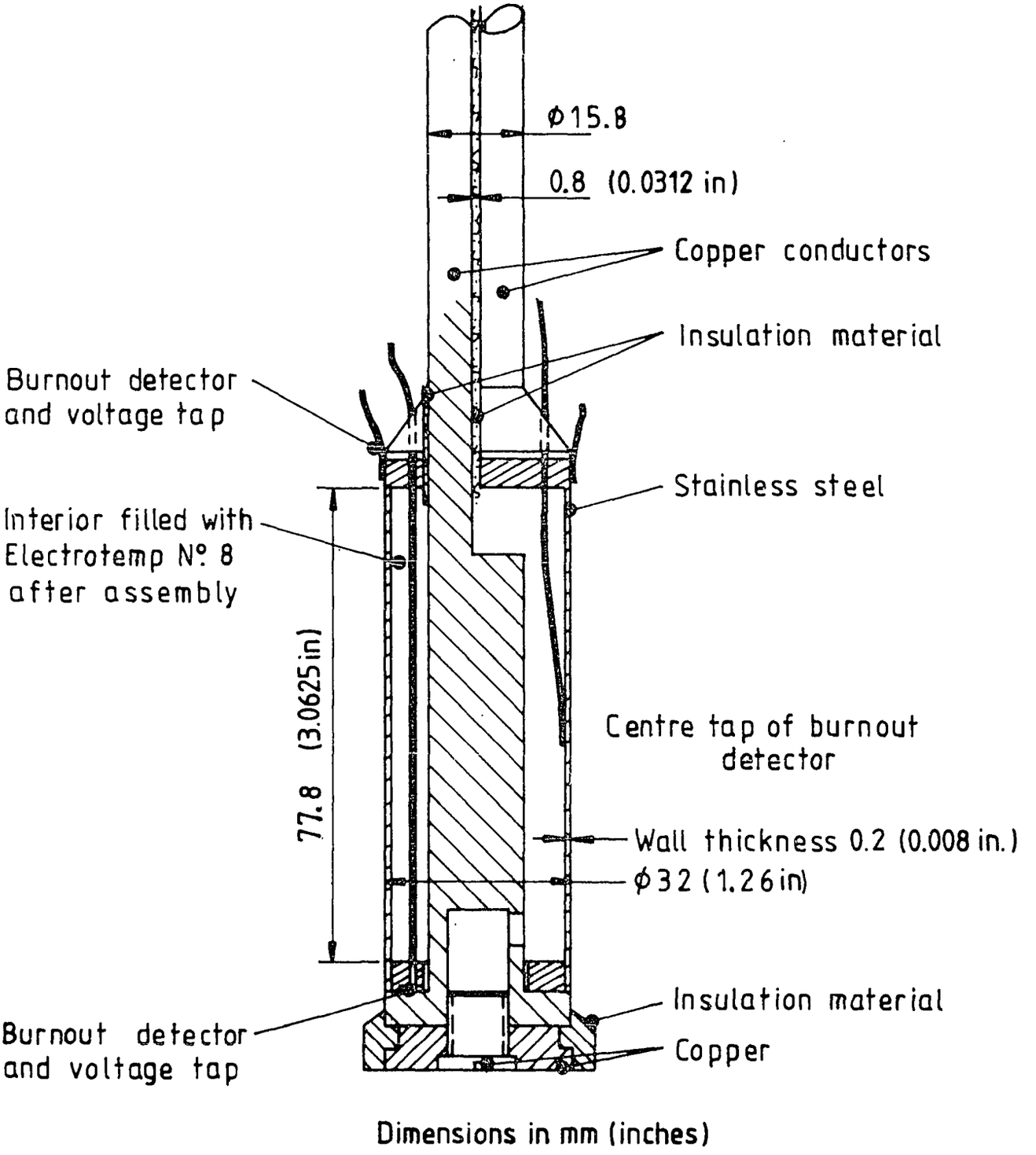

Figure 5 Electrically-heated simulation of irradiation can (whole shell design)

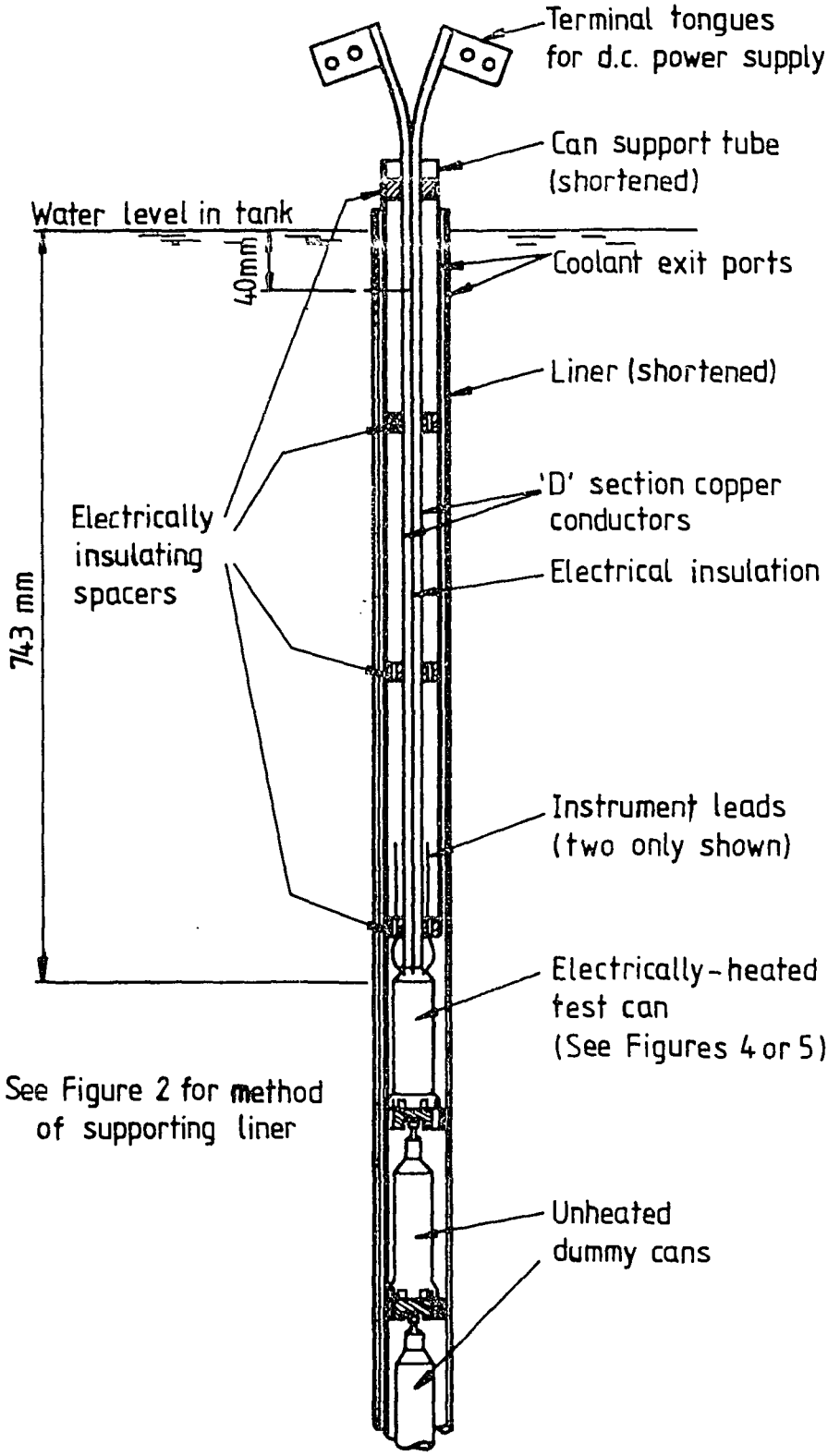

Figure 6 Arrangement of heated can in liner

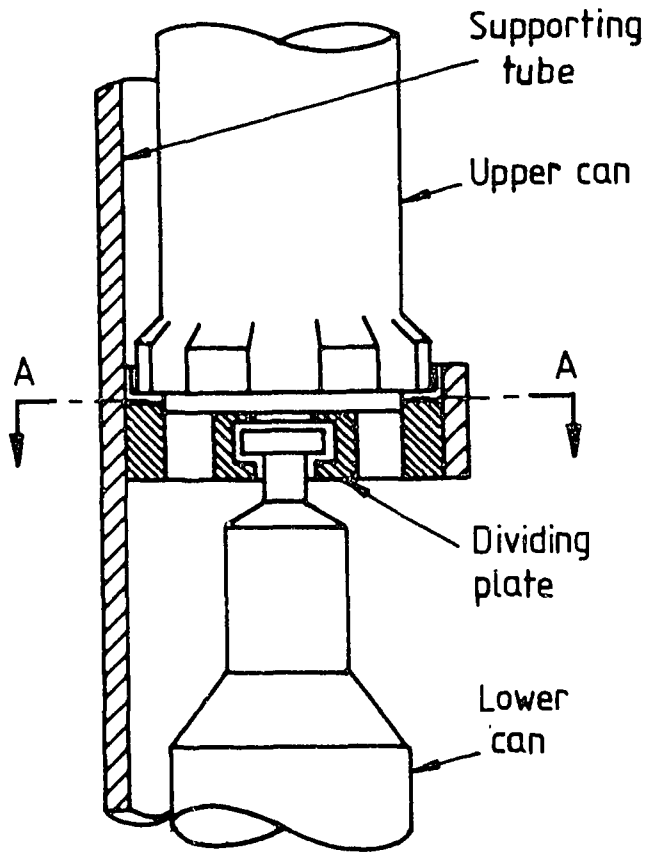

Figure 7a Original dividing plate in can supporting tube

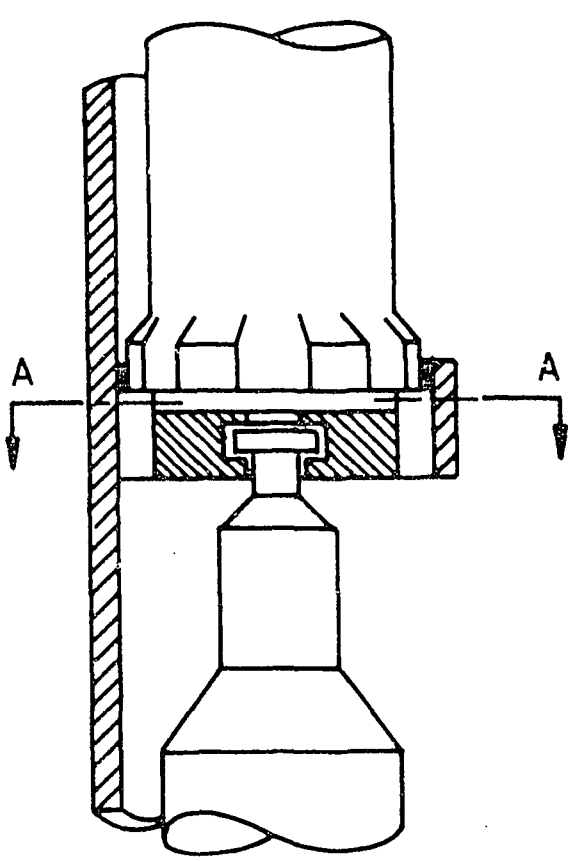

Figure 7b Modified dividing plate in can supporting tube

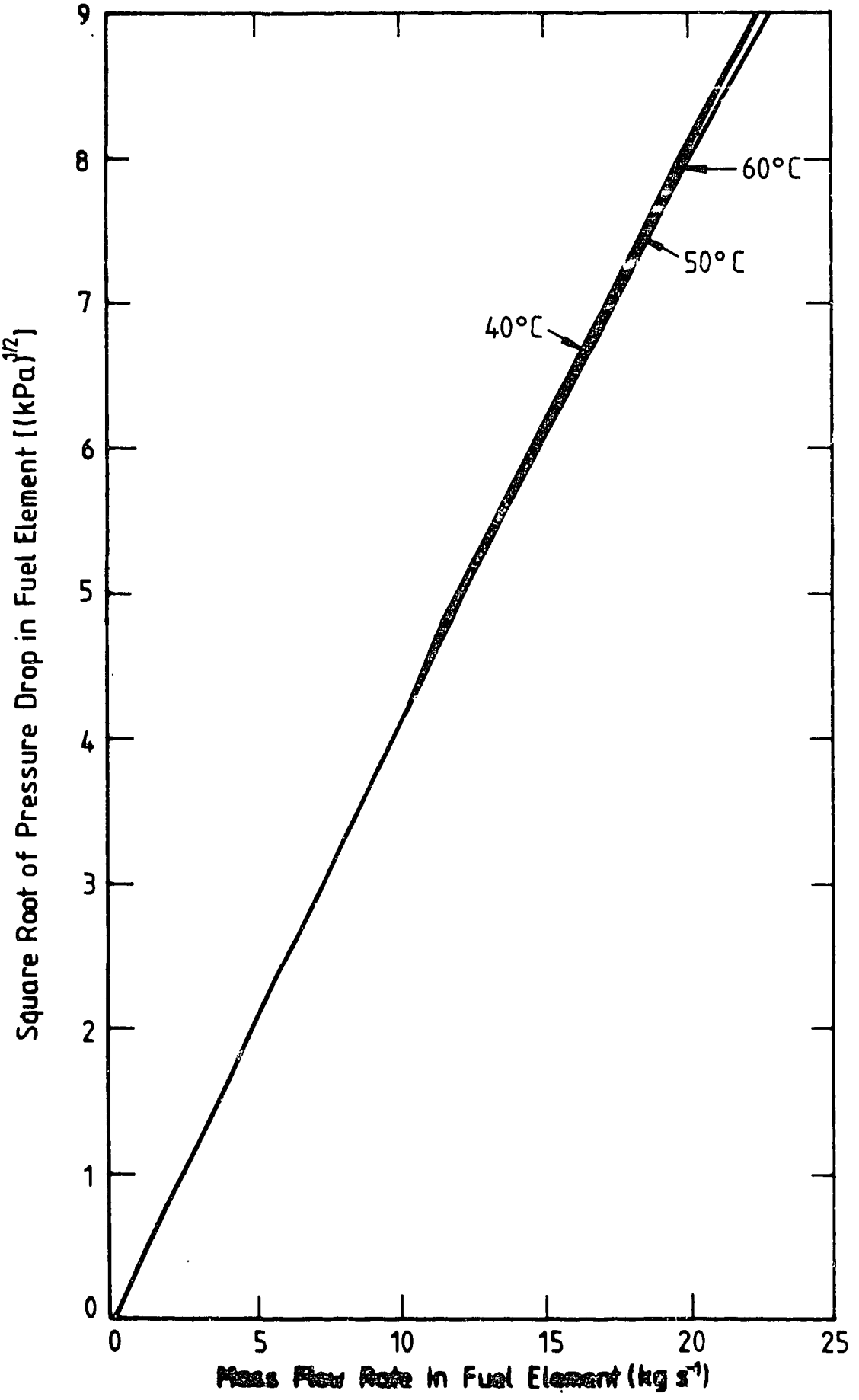

Figure 8 Pressure drop in fuel element

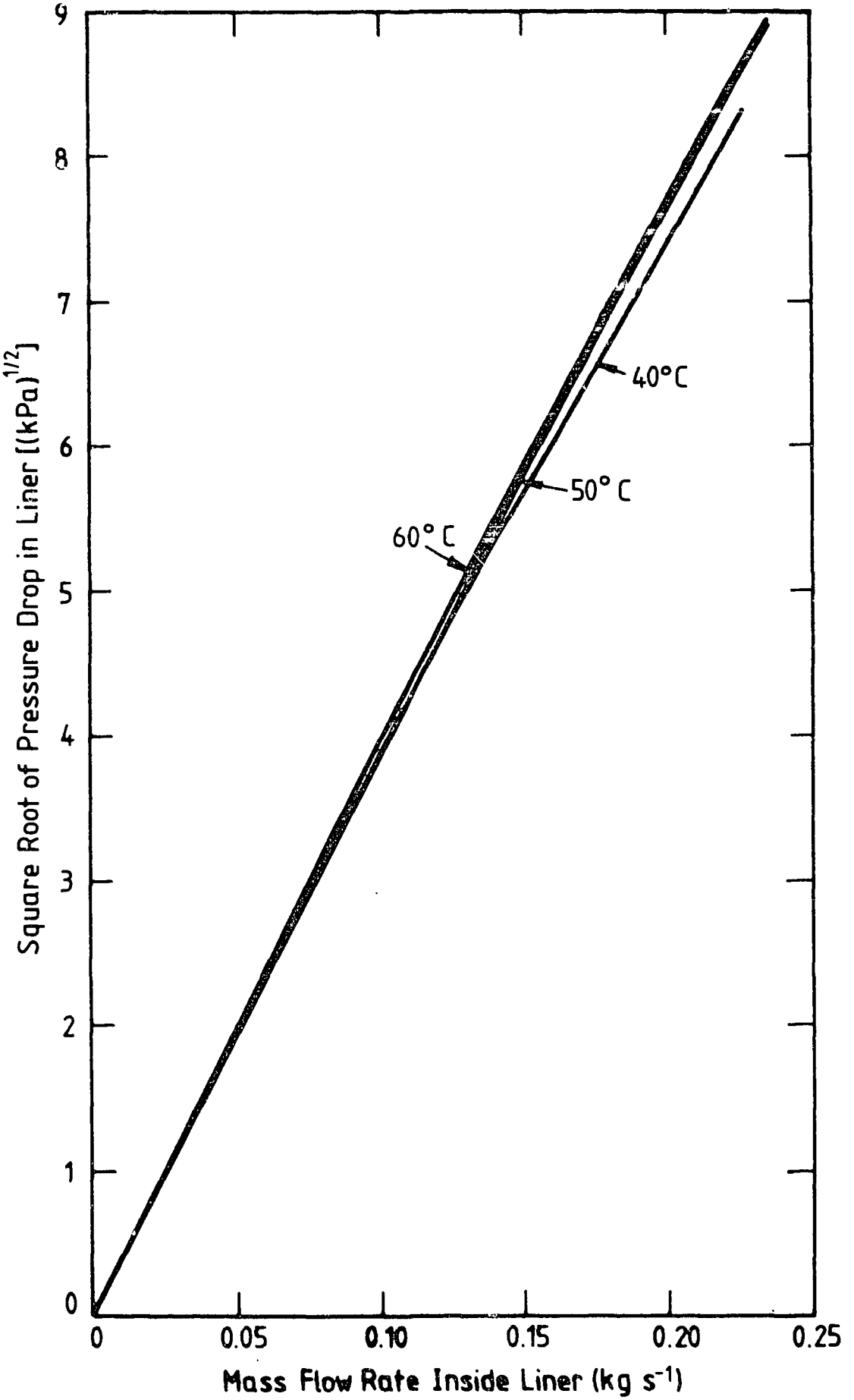

Figure 9 Pressure drop in liner (to point immediately upstream of outlet ports)

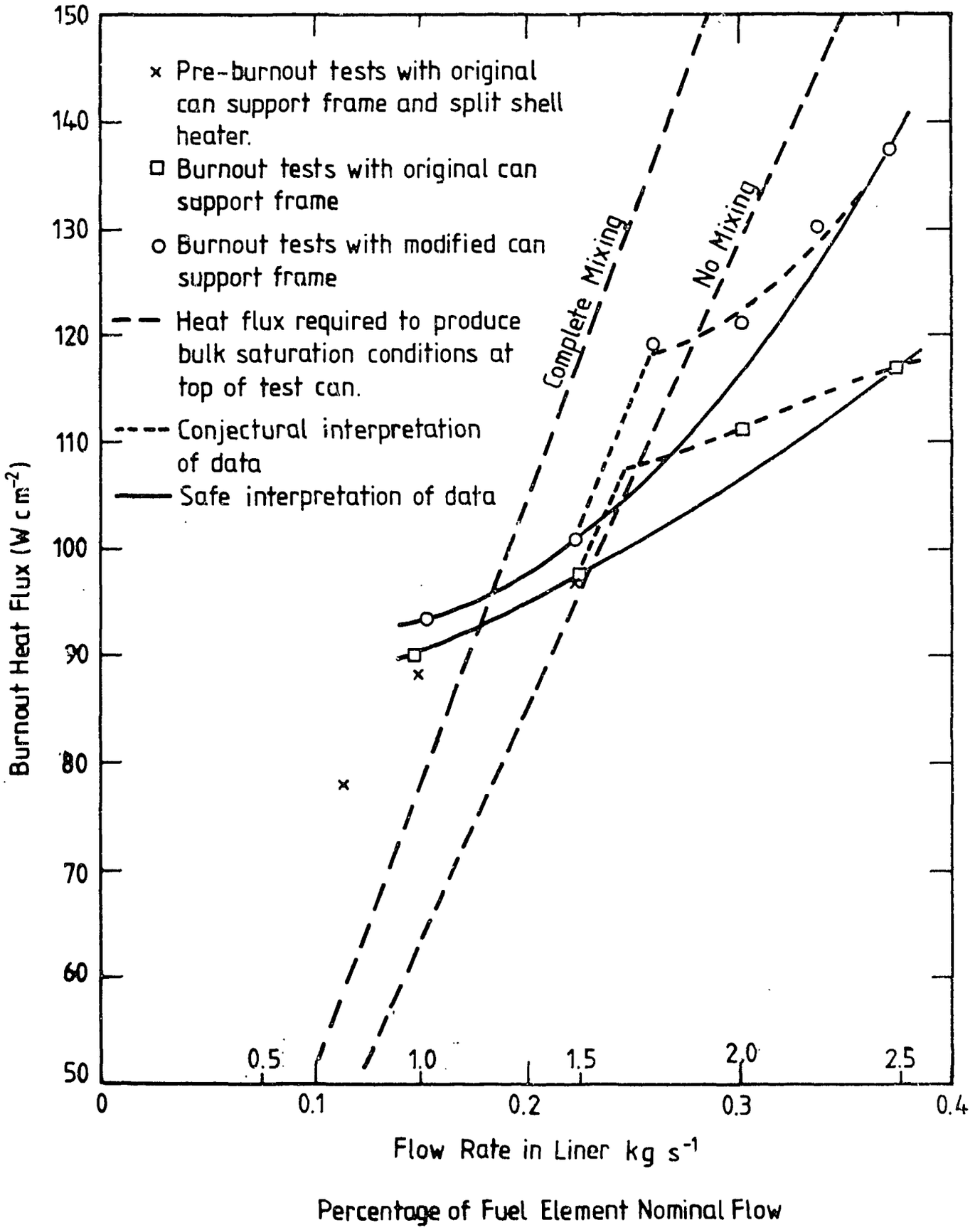

Figure 10 Burnout heat flux variation with coolant flow rate in liner

APPENDIX A

DESCRIPTION OF THE FUEL ELEMENT TEST RIG

The fuel element test rig is designed for the performance of flow tests in demineralised ordinary water on a single full-size dummy fuel element. A diagram of the rig is shown in Figure A1. A dummy fuel element is similar in all respects to a real fuel element assembly for the HIFAR reactor, except for the fuel plates, which are replaced by aluminium plates.

The dummy fuel element and shield plug assembly is supported vertically inside a 400 L stainless steel cylindrical tank of water, open at the top, in a hydraulic simulation of the arrangement of a fuel element in the reactor tank. The spherical seat of the element guide nose is located on the conical seat of a standpipe which passes through the bottom of the tank. The internal dimensions of the standpipe are the same as those of a nozzle in the reactor plenum plate and, like the nozzle, the pipe is fitted with cruciform flow-straightening vanes. The level of water in the test tank is the same as that of heavy water in the reactor aluminium tank. The tank has a side outlet branch near the bottom.

Water is circulated through the dummy fuel element by a 1600 L min^{-1} gunmetal centrifugal pump, which takes water from the tank outlet branch and delivers it to the standpipe, on which the element rests, via 100 mm nominal bore stainless steel pipework. Stainless steel bellows connect the pump to the pipework, to minimise the transfer of vibrations to the test rig. Flow is regulated over a wide range by three valves - a wedge gate valve near the pump discharge for coarse control, a throttle valve in a small-bore bypass around the gate valve for fine control, and a control valve in a small-bore recirculation connection on the pump.

Flow rates are measured with a standard square-edged orifice plate flow meter with corner taps, placed 40 pipe diameters downstream of the gate valve. The pressure difference across the orifice is measured with a calibrated pressure transducer. Three sizes of orifice are used: 66.4 mm diameter for flows between 8 and 26 kg s^{-1}; 11 mm diameter for flows between 0.25 and 0.8 kg s^{-1}; and 6.35 mm diameter for flows less than 0.25 kg s^{-1}.

Water temperature is controlled by heating or cooling, or a mixture of both. The pipe between the gate valve and the flow meter is wrapped, with two thermally insulated 240 V, 3.5 kW heating tapes, each with independent variable voltage control. When cooling is required, a small pump takes

water from the top of the tank, passes it through a fan-cooled finned heat exchanger of about 15 kW capacity, and returns it to the bottom of the tank. Water temperatures are measured with chromel-alumel thermocouples immediately upstream of the orifice plate, in the fuel plate and in the fuel element outlet ports.

To reduce flow disturbances on entry of the coolant to the dummy fuel element, the right-angle pipe bend beneath the tank is followed first by a perforated plate (blockage ratio 0.85) and then by a bundle of 19 mm diameter flow-straightening tubes. Pressure drops between points in the flow circuit are measured with four mercury manometers. The high pressure side of each manometer is connected to a static pressure tapping in the wall of the standpipe, i.e. at entry to the fuel element. The low pressure sides are connected to static pressure tappings in

(i) the wall of the fuel element liner, downstream of the nose cone perforations;

(ii) the wall of the liner, midway between the inlet and outlet perforations;

(iii) the wall of the liner, immediately upstream of the outlet perforations; and

(iv) the wall of the tank, below the water level.

The d.c. power supply for heating the burnout test sections is obtained from a 25 V, 3000 A transformer/rectifier unit, controlled by voltage regulation on the primary side. A trip relay prevents the application of heating power if the water circulating pump is not running. The direct current is indicated by the measured voltage drop across a calibrated shunt.

Thermocouple and pressure transducer output signals, and shunt and test section voltage drops are scanned eight times per minute, converted to temperatures, pressure drop, current, and voltage and displayed and printed by a Kaye 'RAMP' data acquisition system.

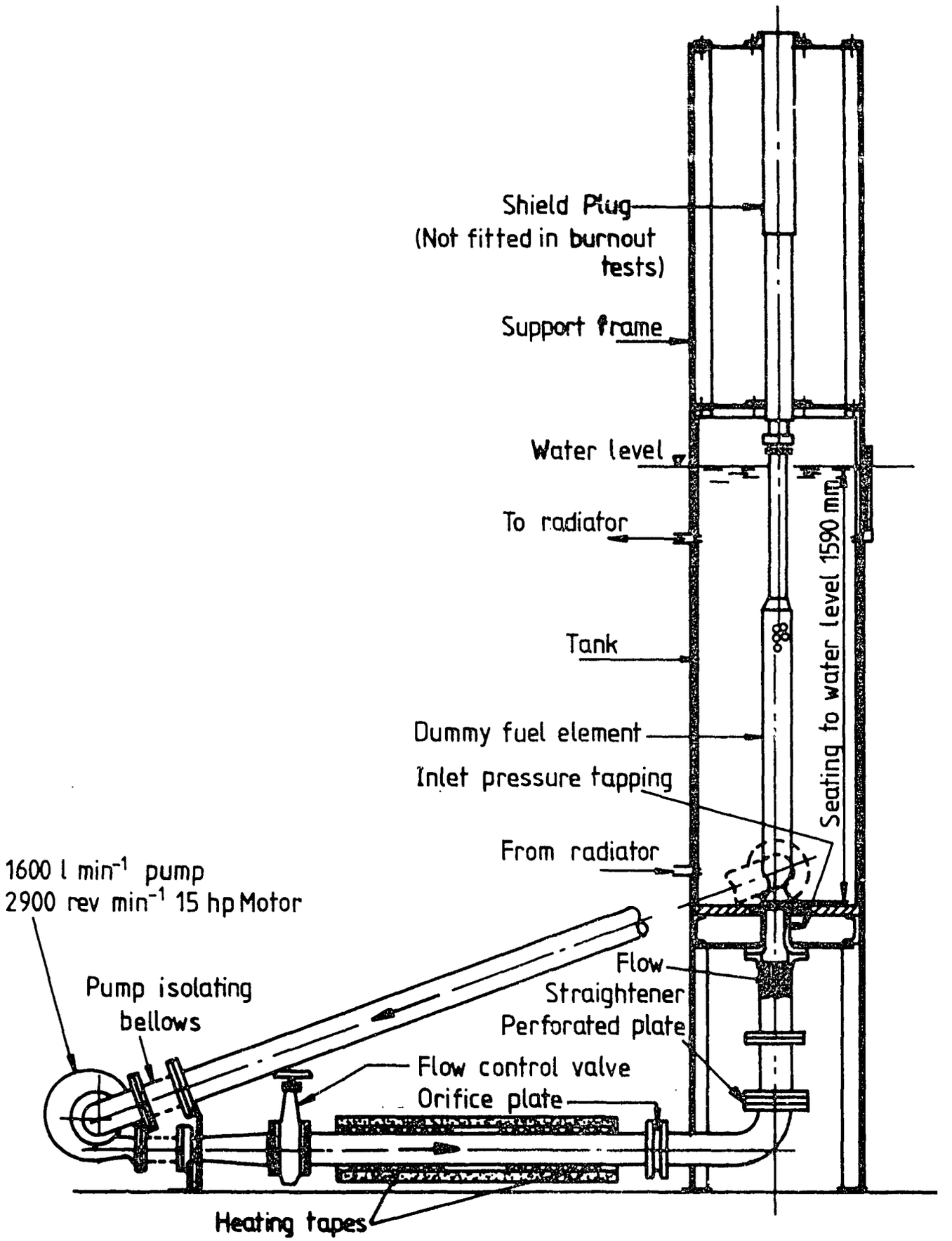

Figure A1 Fuel element test rig

APPENDIX B

STANDARD CONDITIONS OF TEST

In all references to tests or test results the following conditions apply, except where particular differences are specified:

(a) The coolant is demineralised ordinary water.

(b) The pressure at the surface of the water in the tank is atmospheric.

(c) The fuel element, when included in the test section, is a full-size, inactive copy of a Mark 4/5A concentric tube HFE.

(d) The depth of immersion of the top edge of the fuel plates is 750 mm.

(e) The fuel element liner is a standard HFE type 'C' liner, 50.7 mm bore, with standard X183 perforations: inlet, 4 holes of diameter 3.2 mm; outlet, 4 holes of diameter 12.7 mm.

(f) The depth of immersion of the liner outlet perforations is 40 mm.

(g) The liner contains a specimen container, stringer assembly, compartment dividing plate, as shown in figure 7(a), loaded with five cans, the topmost of which (in burnout tests) is an electrically-heated simulation of a specimen can.

(h) The depth of immersion of the top of the heated length of the topmost can is 743 mm.

(i) In burnout tests, the coolant flow rate inside the liner is 0.15 kg s^{-1}.

(j) In burnout tests, the temperature of the coolant entering the topmost support tube compartment is adjusted to conform to the value given by equation (9.1) with

$$T_o = 50° \text{ C}$$
$$C = 4.196 \text{ kJ kg}^{-1} \text{ K}^{-1}$$
$$\alpha = 0.24$$
$$W_g = 1.75 \text{ kW}$$

The equation then reduces to

$$T = 50 + \frac{0.755W + 0.334}{M}$$

This is the temperature attained at the entry to the compartment containing the topmost can when

(i) coolant enters the fuel element at a temperature of 50°C,

(ii) the flow rate inside the liner is M kg s^{-1},

(iii) there are four active cans loaded in the four lowest positions,

(iv) the rate of heat generation in the topmost can is W kW, and

(v) heat is generated in the three lower cans according to the distribution, selected from the table in Appendix C, which produces the lowest proportion in the fourth can.

APPENDIX C

DISTRIBUTION OF FISSION HEATING IN IRRADIATION RIG

by G. Storr

(a) Fission heating (MW) $= \frac{1}{K} \times \frac{\phi_{th}}{10^{13}} \times {}^{235}U$ mass (kg) x depression factor

$K = 2.55$ at 50°C

Flux depression factor $= 0.815$

ϕ_{th} (total thermal flux) $= \phi_w \times \frac{2}{\sqrt{\pi}} \sqrt{\frac{273 + T}{293}} = \phi_w \times 1.185$

ϕ_w = Westcott convention flux - actual flux in HIFAR (n cm^{-2} s^{-1}).

Assume UO_2 pellet mass is 45 grams,

$\therefore$ ^{235}U mass is 0.7418 grams/can.

(b) Can heating - 2 watts per gram Al. can mass = 175.5 grams.

(c) Heating is calculated for can positions A,B,C,D,E, i.e. possible can positions on an X183 rig.

(d) Flux measurements were carried out in program 296 in facility C2 in an element which was well burnt up. It would therefore be expected to be a plausible maximum case limit for flux and hence can heating of UO_2.

TABLE C1

FLUX MEASUREMENTS AND FISSION HEATING

Hours after Start-up (CCA angle)	Target Position	HIFAR recovered Flux ϕ_w (n cm^{-2} s^{-1})	Fission Heating (kW)	Total Heat (kW)
	A	0.405×10^{14}	1.14	1.49
	B	0.680×10^{14}	1.91	2.26
0	C	1.070×10^{14}	3.01	3.36
(~ 14°)	D	1.135×10^{14}	3.19	3.54
	E	1.030×10^{14}	2.89	3.24
	A	0.755×10^{14}	2.12	2.47
	B	0.920×10^{14}	2.58	2.93
350	C	1.150×10^{14}	3.23	3.58
(~ 21°)	D	1.100×10^{14}	3.09	3.44
	E	0.950×10^{14}	2.67	3.02
	A	0.995×10^{14}	2.80	3.15
	B	1.015×10^{14}	2.85	3.20
670	C	1.205×10^{14}	3.39	3.74
(~ 26°)	D	1.095×10^{14}	3.08	3.43
	E	0.925×10^{14}	2.60	2.95